International Journal of Fluid Power 1 (2000) No. 2 pp. 39-47

AN IMPROVED DYNAMIC MODEL OF PNEUMATIC ACTUATORS

J.-C. Maré, O. Geider and S. Colin

Laboratoire de Génie Mécanique, Institut National des Sciences Appliquées de Toulouse,
135 avenue de Rangueil, 31077 Toulouse Cedex 4, France
jean-charles.mare@insa-tlse.fr

Abstract

An improved predictive model of pneumatic jacks is introduced in order to develop a component oriented model library for the numerical prototyping of pneumatic actuators. First, the valve orifices model is derived from the ISO standard as a function of the orifice opening. Then the gas chamber behaviour is modelled using a rigorous theoretical development of conservation laws. Consequently, no assumption is required concerning the evolution of the gas only being considered as ideal. A fix parameter convective model is found acceptable to define the heat exchange between the gas and the jack environment. Finally, a representation model of the internal jack friction is proposed including the influence of pressure and working quadrant on viscous and Coulomb effects. The simulation structure is then presented and the model is validated using a step by step procedure.

Keywords: pneumatic actuator, friction, pneumatic valve, gas chambers, dynamics

This manuscript was received on 3 May 2000 and was accepted after revision for publication on 29 August 2000

1 Introduction

The pneumatic technology is attractive for a wide field of medium force, linear motion actuation applications. It is cheap, rapid and it avoids pollution in the event of external fluid leakage. So, this technology can present a real advantage for positioning systems. Until now, it has been essentially used for pick and place applications despite the efforts made in the development of proportional actuators. One of the main reasons is that the control valve costs generally more than five times the jack price. In such a way, the advantages associated to pneumatic actuation fall down. The second main reason lies in the non linear behaviour that is difficult to predict accurately and to control. It is so hard to obtain simple models for industrial applications.

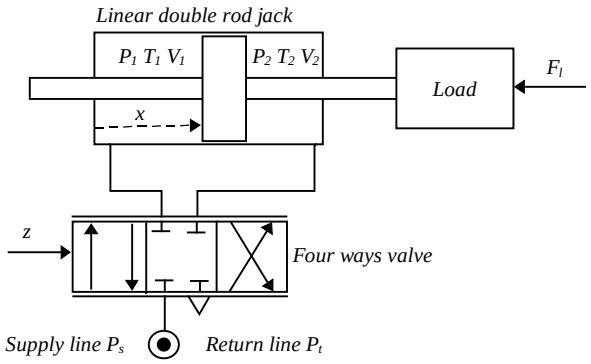

Fig. 1: *Scheme and conventions (four ways valve case)*

Table 1: Main characteristics of the pneumatic actuator

Jack type	3/2 Valve type	4/2 Valve type
CAMOZZI 41M6P	SIRAI L331B12	THOMSON
Piston diameter 32 mm	Nozzle type	Sliding Spool
Rod diameter 12 mm	Diameter 1.6 mm	Spool diameter 6.35 mm
Full stroke 250 mm		Spool stroke 4 mm

In order to solve the problems for industrials interested in proportional pneumatic actuation, research works were performed in these two directions. The work

reported in this paper deals with the improvement in the knowledge of the jack dynamics and the development of an accurate simulation model that could be structured as a component library.

The linear double rod actuator on study, Fig. 1, may be operated in the single effect or in the double effect mode, depending on the experimental conditions. In the first mode a three ways valve controls the gas energy exchanged with chamber 1 while chamber 2 is pressurised at half the supply pressure. In the second mode, an industrial four ways valve drives the two chambers in opposition. The main data concerning the actuator are summarised in Table 1.

2 Accurate Knowledge Model

According to the highly non linear behaviour of pneumatic actuators, it is well established that one cannot built a unique model for both predictive modelling and control design purposes. If the last ones are usually well developed, we consider that the main loss of accuracy in predictive models of pneumatic systems is due to the lack of improved models for variables orifices and gas chambers dynamics. For this reason, a careful work has been done in these directions.

2.1 Compressible Flow through Orifices

The basic model of compressible flow through orifices is built from the Saint Venant equation that gives the gas velocity in a restriction, assuming the gas is ideal, the flow is unidirectional and the upstream gas velocity can be neglected compared with the velocity in the restriction, Comolet (1985). This yields to the common formulation given by the system of Eq. 1 to 3.

If $\frac{P_d}{P_u} > \Omega$, the flow is subsonic so

$$q = s P_u \left\{ \frac{2\gamma}{(\gamma - 1) r T_u} \left[\left(\frac{P_d}{P_u} \right)^{2/\gamma} - \left(\frac{P_d}{P_u} \right)^{\gamma + 1/\gamma} \right] \right\}^{1/2} \quad (1)$$

else the flow is sonic, so

$$q = s P_u \left\{ \frac{\gamma}{r T_u} \left(\frac{2}{\gamma + 1} \right)^{\gamma + 1/\gamma - 1} \right\}^{1/2} \quad (2)$$

The theoretical transition appears when

$$\Omega = \left(\frac{2}{\gamma + 1} \right)^{\frac{\gamma}{\gamma + 1}} \quad (3)$$

This model is particularly convenient for the modelling of ideal nozzles. It is still commonly used for valves orifices, Hong (1995), Kunt et al (1990) Uebong et al (1997), although it does not take into account the effective orifices geometry that produces in practice a critical pressure ratio varying from 0.15 to 0.5 while the theoretical value is 0.52. As described by system 4 and 5, the ISO 6358 standard overcomes these limitations assuming an elliptic subsonic characteristic defined by parameters b and C : the transition between subsonic and

sonic conditions is fixed by parameter b instead of Ω while the conductance of the valve is fixed by parameter C.

$$\text{Subsonic } q = C\,\rho_n\,P_u\sqrt{\frac{T_n}{T_u}}\left\{1-\left(\frac{\frac{P_d}{P_u}-b}{1-b}\right)^2\right\}^{1/2} \quad (4)$$

$$\text{Sonic } q = C\,\rho_n\,P_u\sqrt{\frac{T_n}{T_u}} \quad (5)$$

In the case of variable orifices, the sonic conductance and the critical pressure ratio are identified from experiments as functions of the orifice opening. Given the measured values of pressure, flow and opening, they are obtained by direct identification using the model given by Eq. 5 and 6. Typical data are displayed on Fig. 2 for the valve used in this application, pointing up the 15% spool-bushing overlap that provides null flow around the null opening.

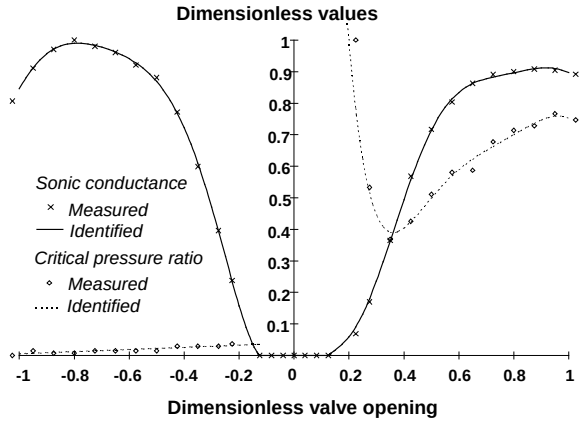

Fig. 2: *Typical characteristic of a 4 ways pneumatic valve*

The lines display the valve simulated characteristic got by curve fitting technique from experimental data.

As the dynamics of flow through orifices is much higher than the ones related to the jack, it is generally assumed that the above model is convenient. Comparing simulation and experiments of the pneumatic actuator proves that this assumption does not introduce any reduction in the actuator model accuracy.

2.2 Gas Dynamics in Jack Chambers

Basic models of pneumatic jacks, Andersen (1967) assumed that the gas evolution is polytropic in each chamber. These models have been progressively improved considering that all evolutions are adiabatic with isentropic conditions for the emptying chamber, Wang et al (1987). More recently, the restriction to a full isentropic model, Kain et al (1973) or isothermal model, Scavarda et al (1994) have been used with success in order to design position controllers. That confirms these assumptions are well suited for position control models.

Unfortunately, such a global description of the chambers thermodynamics is not accurate enough to provide useful predictive models. Rigorously speaking, these assumptions are only valid for a continuous steady mass flow rate. As the mass of the gas varies in each chamber, the simulation results got using this hypothesis may be at variance with experiments. This becomes evident when considering the upper dynamic state variables, like chamber pressure or spool acceleration, that suffer from such a model. Furthermore, the model is generally validated in position closed loop operation that smoothes the modelling error due to the correlation between the control signal and the actual piston position.

This is the reason why the following detailed analysis of the thermodynamics of gas chambers has been developed with great care.

For each chamber, the control volume is defined by Fig. 3, considering there is no leakage across the piston. It is associated with three conservative quantities: mass, energy and momentum.

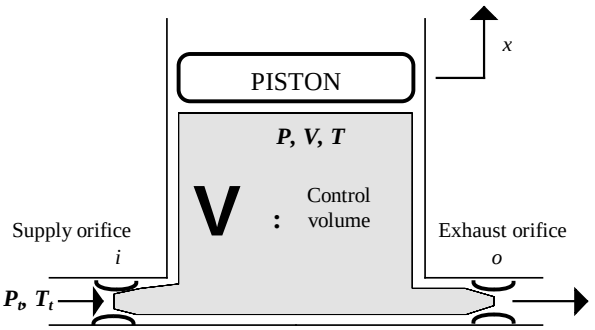

Fig. 3: *Control volume*

The conservation law is applied to the control volume for each of these variables using the surfacic or volumic average values as introduced in the Appendix and neglecting the gas viscosity and weight.

2.2.1 Conservation of Energy

According to Eq. 40, the conservation balance applied to the total energy is given by Eq. 6.

$$m\frac{\delta\left[e+\frac{V^2}{2}\right]}{\delta t}+\left[e+\frac{V^2}{2}\right]\frac{\delta m}{\delta t}=\frac{d}{dt}\int_V \rho(e+\frac{V^2}{2})\,d\varpi$$

$$+\left[\left|(e+\frac{V^2}{2})_i\right|\right]q_i-\left[\left|(e+\frac{V^2}{2})_o\right|\right]q_o \quad (6)$$

The first term of the right hand side can be developed as eq. (7) introducing the outcoming power related to pressurised gas and thermal exchanges with the environment.

$$\frac{d}{dt}\int_V \rho\left(e+\frac{V^2}{2}\right)d\varpi=\int_\Sigma -P\vec{V}\cdot\vec{n}\,ds-\Phi \quad (7)$$

The surface integral can be written in the discrete form as Eq. 8 considering the average values, Colin (1992), defined by Eq. 36.

$$\int_{\Sigma} -P\vec{V}\cdot\vec{n}\,ds = -\left\langle \left| P_p\, V_p \right| \right\rangle s_p$$

$$+\left\langle \left| P_i\, V_i \right| \right\rangle s_i - \left\langle \left| P_o\, V_o \right| \right\rangle s_o \qquad (8)$$

In order to minimise the model parameters to be identified and to improve the robustness of the actuator model, the heat exchange between the gas and the jack environment is represented by Eq. 9 as an average equivalent convection effect.

$$\Phi = \varphi\, s_e \left([T] - T_a \right) \qquad (9)$$

The energy conservation balance is then derived from Eq. 7 to 9 taking into account the following remarks :

- the gas, assumed to be ideal, verifies the Eq.10 and 11

$$P = \rho\, rT \qquad (10)$$

$$c_p = c_v + r \ \ (c_p \text{ et } c_v \text{ are constant}) \qquad (11)$$

- the Reynolds number is sufficiently high in the control orifices. So, the gas velocity can be considered as uniform in the whole input or output sections.

- the control orifices are modelled using the ISO 6358 Standard. The quasi static evolutions between the upstream tank and the input section and between the chamber and the output section conserve energy. This yields to Eq. 12 and 13.

$$c_p\, T_i + \frac{V_i^2}{2} = c_p T_t \qquad (12)$$

$$c_p\, T_o + \frac{V_o^{\,2}}{2} = c_p\, T + \frac{V^2}{2} \qquad (13)$$

In practice, the piston speed never exceeds a few meter per second. For that reason, we can consider that the gas kinetic energy is much lower than the gas internal energy in the chamber. The last term of Eq. 13 can so be dropped.

Finally, the useful form of the energy conservation law applied to the control volume is given by Eq. 14.

$$m\frac{\delta[T]}{\delta t} + [T]\frac{\delta m}{\delta t} = -\frac{1}{c_v}\left\langle \left| P_p \right| \right\rangle V_p s_p - \frac{1}{c_v}\varphi\, s_e \left([T] - T_a \right)$$

$$+\gamma\, T_t\, q_i - \gamma\, [T]\, q_o \qquad (14)$$

2.2.2 Conservation of Mass and Momentum.

The mass and momentum balances, Eq. 15 and 16, are written directly from Eq. 40.

$$\frac{\delta m}{\delta t} = q_i - q_o \qquad (15)$$

$$m\frac{\delta[V]}{\delta t} + [V]\frac{\delta m}{\delta t} = \frac{d}{dt}\int_V \rho V\, d\varpi + \left[|V_i| \right] q_i - \left[|V_o| \right] q_o \qquad (16)$$

In the particular case on study, the average gas velocity in the chamber is not supposed to be computed as its effect has been neglected in Eq. 13. As a consequence, the momentum balance is useless.

2.3 Piston Dynamics

The transmission stiffness between the piston and the load is supposed to be negligible compared with the pneumatic stiffness. So, the Newton's second law applied to the piston - load assembly is written as eq. (17).

$$M\frac{d^2x}{dt^2} = \left\langle \left| P_{p1} \right| \right\rangle s_1 - \left\langle \left| P_{p2} \right| \right\rangle s_2 + P_a\left(s_{r1} - s_{r2}\right) - F_l - F_f \qquad (17)$$

A lot of experiments have been performed in order to determine the jack friction characteristic, Armstrong-Hélouvry (1991). For this application, the most efficient procedure was found when the motion of the pneumatic jack is forced by an external actuator controlled in position. In addition, each pressure of the jack chamber is kept constant by direct connection to a high volume accumulator. The inertial force is calculated from the total mobile mass and the jack acceleration that is got by an off-line procedure from the position sensor signal. Finally, the friction force is calculated using Eq. 17 from the measured values of the jack position, the chamber pressures and the transmitted force. As displayed by Fig. 4, dominant Coulomb and viscous effects were pointed up but no significant Dahl or Stribeck effects were observed. Consequently, the friction model structure reduces to Eq. 18 when sliding.

$$F_f = K_v\frac{dx}{dt} + F_C \qquad (18)$$

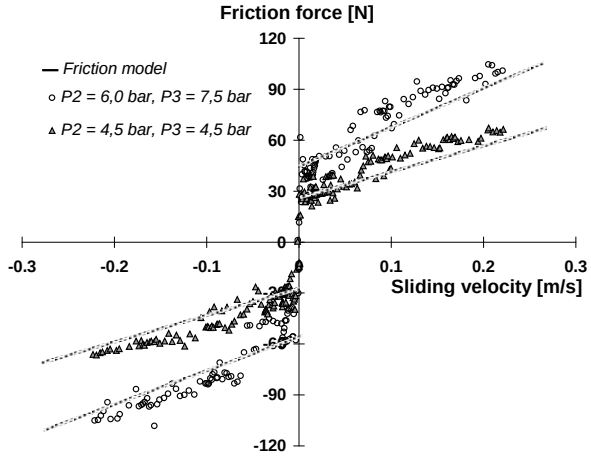

Fig. 4: *Typical friction data*

When sticking or at null speed, the friction force balances the external forces as far as it is less than the Coulomb value.

It has been found that the chamber pressures have a great influence on the friction level due to the internal and external sealing design. In that way, the friction parameters have been made dependant on the chamber pressures using Eq. 19 and 20.

$$K_v = K_{v2}\left[P_2\right] + K_{v3}\left[P_3\right] \qquad (19)$$

$$F_C = F_{C2}\left[P_2\right] + F_{C3}\left[P_3\right] \qquad (20)$$

The four coefficients have been estimated from various experiments, showing that values were different for positive or negative sliding speed. This is due to the quadrant effect, Maré (1993), that changes the friction force when the load moves against or with the pressure force, for same modulus of pressure and speed conditions.

3 Model Simulation

The pneumatic actuator model is built combining Eq. 4 and 5 for each working orifice, Eq. 14 and 15 for each piston chamber and Eq. 17 to 20 for the piston-load assembly. The pressure continuity is ensured assuming the pressure on the piston surface is equal to the corresponding chamber pressure

$$\left\langle \left| P_p \right| \right\rangle = \left[P\right] \qquad (21)$$

that combines with Eq. 10 to give

$$\left[P\right] = \left\langle \rho \right\rangle r\left[T\right] \qquad (22)$$

Finally, the gas pressure, temperature and mass state variables are linked using Eq. 38 and 22 to yield

$$\left[P_2\right] = \frac{m_2}{s_2\,x + v_{m2}} r\left[T_2\right] \qquad (23)$$

$$\left[P_3\right] = \frac{m_3}{\left(l - s_3\right)x + v_{m3}} r\left[T_3\right] \qquad (24)$$

that complete the actuator model. At this time, the above sixth order model does not include the valve spool dynamics that requires further modelling efforts to be simulated with high accuracy.

The simulation program is structured in order to develop a component library as defined on Fig. 5. It has been computed using the ACSL software, ACSL (1995). All the model discontinuities (like friction commutation between sliding and sticking motion) have been handled with care thanks to the schedule facility that performs a backstep method to manage the discontinuity.

4 Model Validation

The actuator on study has been equipped for later digital control application. The piston position is measured using a self conditioning LVDT while the chamber pressures are monitored with high response strain gage sensors. The sensors signal data are recorded using a Keithley DAS 1600, 12 bit acquisition board for personal computer. The entire acquisition procedure is designed so that the measurement phase lags are minimised. The real-time acquisition program is written at the register level using a pipeline technique that emulates a burst mode even at high sampling rates. For the same reason, the velocity signal has been obtained from position data by off-line acausal filtered derivation.

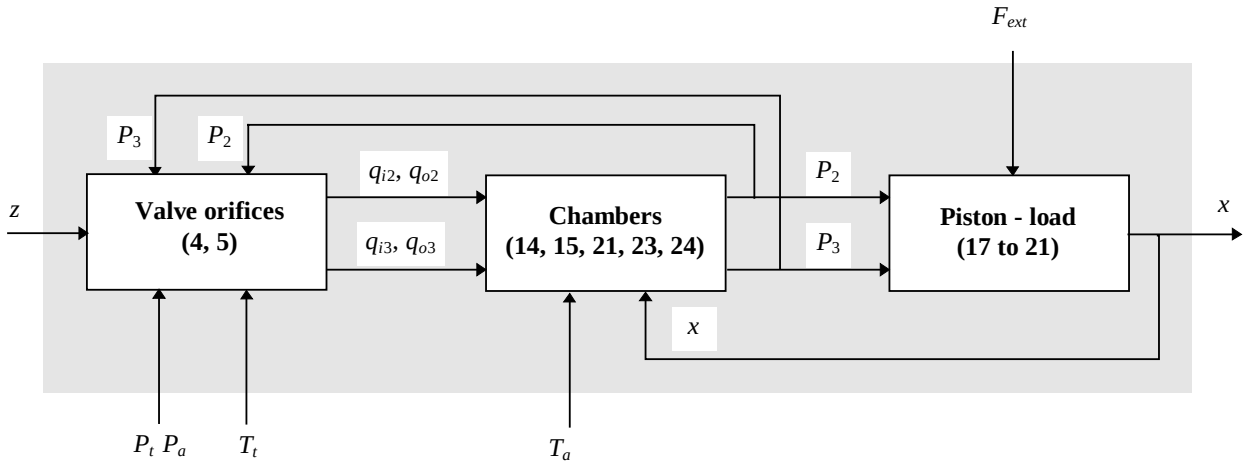

Valve orifices :	*Chambers :*	*Piston load :*
Parameters b *and* C *functions*, ρ_n, T_n	C_v, γ, s_e, φ, s_{p2}, s_{p3}, v_{m2}, v_{m3}, l, r	K_{v2}, K_{v3}, F_{C2}, F_{C3}, s_{p2}, s_{p3}, s_{t2}, s_{t3}, M
State variables None	m_2, m_3, T_2, T_3	x, dx/dt

Fig. 5: Model structure of pneumatic jack

In order to validate the proposed model progressively, a step by step procedure has been performed. At the first level, the valve orifices have been experienced to check the validity of the quasi-static hypothesis. Then the valve has been associated to the jack whose piston was locked. In such a way, various step valve experiments where carried out to validate the chamber model. As shown by Fig. 6 and 7, the pressure evolution is predicted accurately by simulation, even when the chamber volume is changed from its lowest to its highest value (change ratio up to 25). This proves that the assumption written as Eq. 9 was applicable: the heat exchange between the chamber and the ambience can be modelled as convective, using a constant convection coefficient.

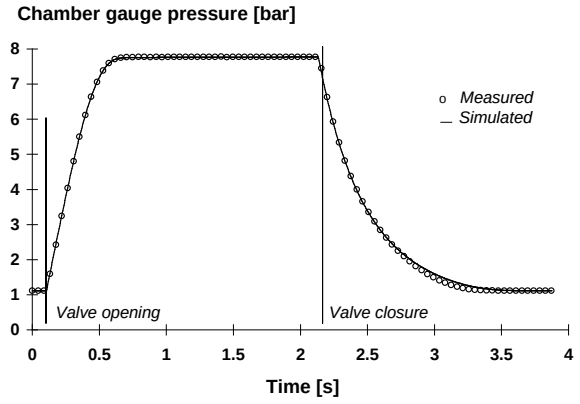

Fig. 6: *Chamber response at maximum volume*

The actual simulation accuracy is compared on Fig. 8 with those got using isothermal and adiabatic assumptions. It can be noticed that the isothermal and adiabatic assumptions produce equivalent errors when the gas is compressed while the proposed model is very efficient in error reduction. In the expansion case, the isothermal assumption looks a little more accurate. Once again, the proposed model reduces the modelling error but with a lesser improvement.

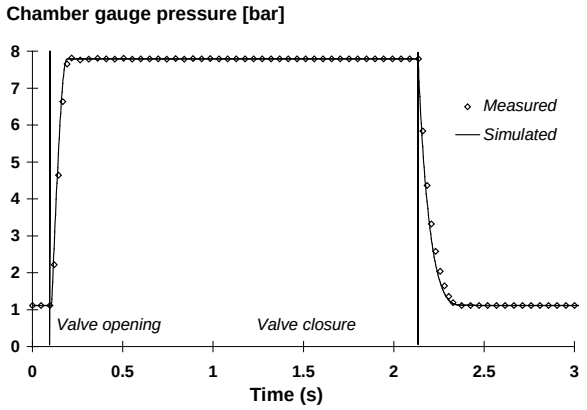

Fig. 7: *Chamber response at minimum volume*

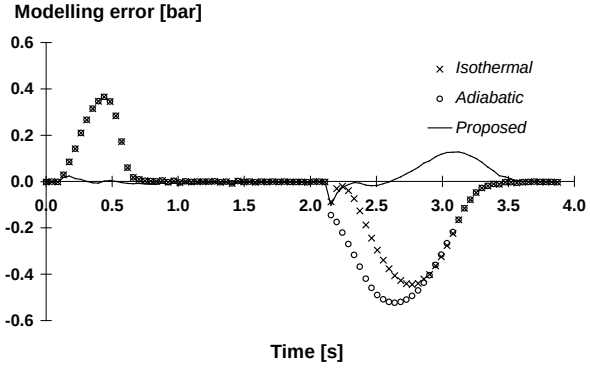

Fig. 8: *Comparison of models accuracy referred to Fig. 6 for maximum volume chamber*

The mean relative error between experiments and simulation, defined by Eq. 25 is summarised in Table 2. For both extreme conditions, it is kept behind 2.01% when the proposed model is used. It reaches 9% for the isothermal model and 13% for the adiabatic one. The prediction capability is so improved by a factor up to 6.

$$\varepsilon = \sqrt{\frac{\sum_{\text{data}} \left(P_g - P_s\right)^2}{\sum_{\text{data}} P_s^2}} \qquad (25)$$

Table 2: Comparison of models accuracy

	Chamber volume	Actual Model Error	Adiabatic model error	Isothermal model error
Valve	min.	0.95	0.94	0.94
opens	max.	1.22	2.82	2.82
Valve	min.	1.14	6.10	4.64
closes	max.	2.01	13.08	8.87

The ultimate validation is performed when the piston is attached to an inertial load and piloted in open loop. So, the effective valve opening is made of two successive pulses ordering the jack extension then the jack retraction. Fig. 9a and 9b display the simulated

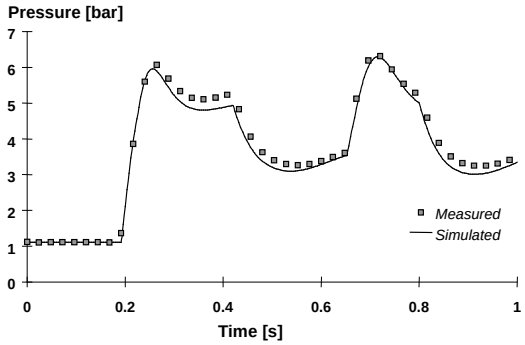

Fig. 9 a: *Single effect operation*
Extension ordered at $t = 0.18\ s$ *and* $t = 0.62\ s$,
Retraction ordered at $t = 0.38\ s$ *and* $t = 0.76\ s$

b)

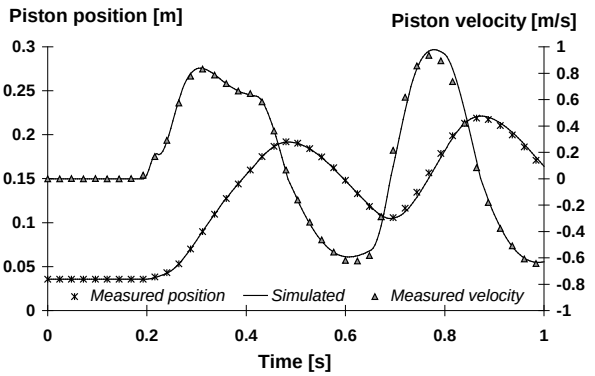

Fig. 9 b: *Single effect operation:*
Extension ordered at $t = 0.18\ s$ *and* $t = 0.62\ s$,
Retraction ordered at $t = 0.38\ s$ *and* $t = 0.76\ s$

and measured responses when the jack is operated in the single effect mode using a three ways valve. Fig. 10 is related to the double effect mode operated with a four ways valve.

It is shown that the modelling error is kept small for all state variables. Considering the low frequency behaviour, the open loop operation is very severe with respect to the model validation. Indeed, the piston position is deduced from the chamber pressures by a double integration and only little physical feedback generated by friction. However, no significant drift is observed excepted local deviations for the pressure signal. The dynamic component is likewise correctly predicted although the excitation spectrum is rich thanks to the step valve opening.

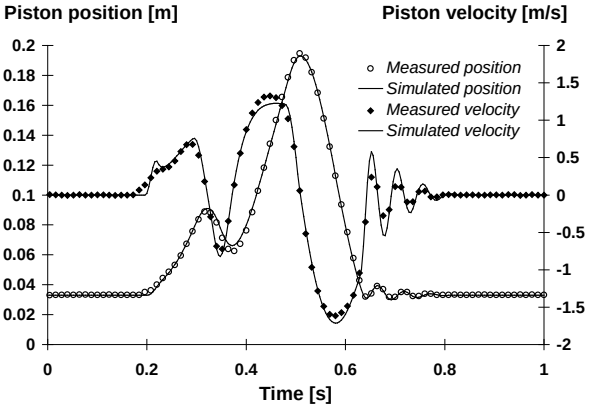

Fig. 10: *Double effect operation*
Extension ordered at $t = 0.18\ s$ *and* $t = 0.62\ s$,
Retraction ordered at $t = 0.28\ s$ *and* $t = 0.564\ s$

The predicted temperature in the double effect operation mode is plotted on Fig. 11. The gas temperature evolution in the chambers has not been checked because no sensors were found to monitor such rate of change. However, the simulated values have been found consistent with those measured in Shimada (1994) where the maximum piston velocity was only 0.3 m/s and the maximum pressure was 0.5 MPa.

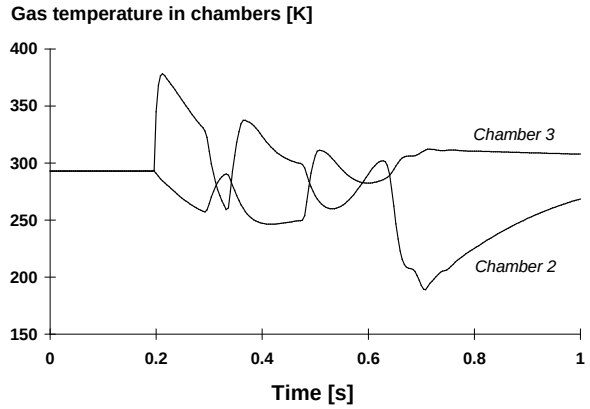

Fig. 11: *Gas temperature in the double effect mode*

5 Conclusion

An improved predictive model of pneumatic jacks has been introduced in order to perform numerical prototyping of pneumatic actuators. This has been achieved balancing theoretical developments, standard models and representation models from experiments. The valve orifices are modelled and identified using the ISO standard while the jack friction takes into account the effect of the working pressure on the Coulomb and viscous friction effects. Rigorous theoretical developments are proposed for conservation principles that allow an internal modelling of the thermodynamics effects concerning the gas that is considered as ideal. As a consequence, no assumption is required concerning the gas evolution in the chambers. The step by step validation procedure has shown excellent correlation between simulation and experiments once only a few model parameters are identified. However, it must be kept in mind that the dissipation effects due to the seals friction are very sensitive to service life and time that may require a statistical processing to predict the control robustness safely.

This model has been employed successfully to the numerical design of position controllers, using a variable structure control of the valve that does not require an accurate model of its dynamics.

Appendix

In the case of gas chambers as encountered in pneumatic actuators, the flow may be transient and the geometry of the control volume changes when the piston moves. On the one hand, the conservation principle applies basically to a fluid domain that is followed in its motion. On the other hand, the control volume is easily defined using the physical envelope enclosing the gas, giving the useful conservation balance. So, a rigorous application of the conservation principle is complex and requires to elaborate a link between these two considerations.

The modelling of a gas volume is based upon the conservation of three quantities

- the mass

$$m = \int_V \rho \, d\varpi \tag{26}$$

- the total energy

$$E = \int_V \rho \left(e + \frac{V^2}{2} \right) d\varpi \tag{27}$$

- the momentum

$$Q = \int_V \rho V \, d\varpi \tag{28}$$

They can all be expressed using the unique form in Eq. 29 where X is equal to unity for mass, to V for

momentum and to $e+V^2/2$ for energy.

$$\int_V \rho\, X\, d\varpi \tag{29}$$

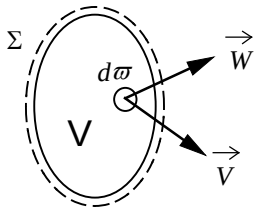

Fig. 12: *The control volume*

As displayed by Fig. 12, it is assumed that at time *t*, the control volume V defined by the gas physical envelope ϖ is superposed to the fluid domain to which the conservation principle is applied. The infinitesimal element of the control volume boundary $d\varpi$ is assumed to have an absolute velocity $\vec{W}$ while the fluid flows through this surface with an absolute velocity $\vec{V}$.

The absolute derivative of the conservative quantity in the control domain can be developed as the common fluid mechanics Eq. 30 using the Ostrogradski theorem.

$$\frac{d}{dt}\int_V \rho\, X\, d\varpi = \int_V \frac{\partial}{\partial t}(\rho\, X)\, d\varpi + \int_\Sigma \rho\, X\, \vec{V}\cdot\vec{n}\, d\sigma \tag{30}$$

The particular derivative related to the velocity of the control volume boundary, is given by Eq. 31.

$$\frac{\delta}{\delta t}\int_V \rho\, X\, d\varpi = \int_V \frac{\partial}{\partial t}(\rho\, X)\, d\varpi + \int_\Sigma \rho\, X\, \vec{W}\cdot\vec{n}\, d\sigma \tag{31}$$

This expression is especially interesting for jacks modelling because it links the gas evolution and the piston motion. Unfortunately, some terms cannot be evaluated directly and require further developments. However, the general conservation law applied to the control volume can be expressed subtracting Eq. 30 from Eq. 31 :

$$\frac{\delta}{\delta t}\int_V \rho\, X\, d\varpi = \frac{d}{dt}\int_V \rho\, X\, d\varpi + \int_\Sigma \rho\, X\left(\vec{W}-\vec{V}\right)\cdot\vec{n}\, d\sigma \tag{32}$$

At this stage, it is necessary to introduce the average surfacic and volumic values as defined by Eq. 33 to 36.

Volumic mass weighted average:

$$\left[X\right] = \frac{\int_V \rho\, X\, d\varpi}{\int_V \rho\, d\varpi} \tag{33}$$

Volumic volume weighted average:

$$\left\langle X\right\rangle = \frac{\int_V X\, d\varpi}{\int_V d\varpi} \tag{34}$$

Surfacic mass weighted average:

$$\left[\left|X\right|\right] = \frac{\int_\Sigma \rho\, X\, d\sigma}{\int_\Sigma \rho\, d\sigma} \tag{35}$$

Surfacic volume weighted average :

$$\left\langle\left|X\right|\right\rangle = \frac{\int_\Sigma X\, d\sigma}{\int_\Sigma d\sigma} \tag{36}$$

According to Fig. 3, the last right hand term of Eq. 32 can be developed on the useful boundaries as

$$\int_\Sigma \rho\, X\left(\vec{W}-\vec{V}\right)\cdot\vec{n}\, d\sigma = \int_{\Sigma_p} \rho\, X\left(\vec{W}-\vec{V}\right)\cdot\vec{n}\, d\sigma$$

$$+\int_{\Sigma_i} \rho\, X\left(\vec{W}-\vec{V}\right)\cdot\vec{n}\, d\sigma + \int_{\Sigma_o} \rho\, X\left(\vec{W}-\vec{V}\right)\cdot\vec{n}\, d\sigma \tag{37}$$

As the envelope and the fluid velocity are identical on the piston surface, the first right hand term is null. For both incoming and outcoming sections, the envelope velocity is null and the fluid velocity profile is flat due to a very high value of the Reynolds number.
Finally, the gas mass Eq. 38

$$m = \left\langle\rho\right\rangle \int_V d\varpi \tag{38}$$

and the gas mass flow rate Eq. 39

$$q = \left\langle\left|\rho\right|\right\rangle sV \tag{39}$$

can be introduced explicitly to give the required conservation Eq. 40 in the average form.

$$m\frac{\delta\left[X\right]}{\delta t} + \left[X\right]\frac{\delta m}{\delta t} = \frac{d}{dt}\int_V \rho\, X\, d\varpi + \left[\left|X_i\right|\right]q_i - \left[\left|X_o\right|\right]q_o \tag{40}$$

The useful equation is then established replacing the first term of the right hand side by the common balances related to the concerned conservative quantity.

Nomenclature

b	Critical pressure ratio	
C	Sonic conductance	[m^3/s/Pa]
c_p	Specific heat at constant pressure	[J/K/kg]
c_v	Specific heat at constant volume	[J/K/kg]
e	Internal energy	[J/kg]
F	Force	[N]
K	Friction coefficient	[kg/s]
l	Piston stroke	[m]
m	Mass of gas	[kg]
M	Mass of piston - load assembly	[kg]
$\vec{n}$	Normal unity vector	
P	Absolute pressure	[Pa]
q	Mass flow rate	[m^3/s]
r	Gas constant	[J/K/kg]

s	Section	[m^2]
t	time	[s]
T	absolute temperature	[K]
V	fluid velocity	[m/s]
v	volume	[m^3]
$\mathcal{V}$	control volume	
W	envelope absolute velocity	[m/s]
x	piston position null when fully	[m]
z	valve opening	[m]
φ	equivalent convection coefficient	[$W/m^2/K$]
ε	mean relative error	
Φ	heat exchanged power	[W]
γ	ratio of specific heats	
ρ	density	[kg/m^3]
Ω	theoretical critical pressure ratio	
ϖ	surface element	
$\delta/\delta t$	particular time derivative	
d/dt	absolute time derivative	
$\partial/\partial t$	partial time derivative	

Subscripts

a	ambient
C	Coulomb
d	downstream
e	exchange
f	friction
g	gauged from experiment
i	incoming
l	load
m	dead
n	normal conditions
o	outcoming
p	piston
r	rod
s	simulated
t	tank
u	upstream
v	viscous

References

ACSL 1995. *Advanced Continuous Simulation Language reference manual*. Mitchel and Gauthier Associates Inc, Concord, MA, USA.

Andersen, B. W. 1967. *The analysis and design of pneumatic systems*. John Willey and Sons.

Armstrong - Hélouvry, B. 1991. *Control of machines with friction*. Kluwer academic publishers.

Colin, S. 1992. *Etude et modélisation en écoulements compressibles des systèmes potentiométriques de type buse palette*. Thèse, Institut National Polytechnique de Toulouse.

Comolet, R. 1985. *Mécanique expérimentale des fluides*. Tome 1, Masson.

Hong, Z. 1995. Intelligence in pneumatic servo positioning axis. *The fourth Scandinavian International Conference on Fluid Power*, September, Tampere, pp. 556-568.

Kain, J. and **Wartelle, C.** 1973. Dynamique des vérins pneumatiques. *Les mémoires du CETIM*, n°17, Septembre.

Kunt, C. and **Singh, R. A.** 1990. Linear time varying model for on-off valve controlled pneumatic actuators. *Transactions of the ASME*, vol 112, December, pp. 740-747.

Maré, J. C. 1993. *Contribution à la modélisation, la simulation, l'identification et la commande d'actionneurs électrohydrauliques*. Thèse d'état, Université Claude Bernard, Lyon.

Scavarda, S. and **Richard, E.** 1994. Non - linear control of electropneumatic and electrohydraulic servo drives: a comparaison. *11. Aachener Fluidtechnisches Kolloquium*, March, Aachen, pp. 223 - 236.

Shimada, K. 1994. Temperature measurement of pneumatic cylinder in stat of actuation and estimation on temperature variation. *The Fourth International Symposium on Fluid Control, Fluid Measurement and Visualisation*, Cert Onera, Toulouse.

Uebong, M. and **Vaughan, N. D.** 1997. On linear dynamic modelling of pneumatic servo system. *The Fifth Scandinavian International Conference on Fluid Power*, May, Linköping, pp. 363-378.

Wang, Y. T. and **Singh R.** 1987. Frequency response of a nonlinear pneumatic system. *Transaction of ASME, Journal of Applied Mechanics*, vol 54, March, pp. 209 - 214.

JEAN-CHARLES MARÉ
Mechanical engineer diploma from INSA Toulouse in 1982. He spent one year in industry as aerospace testbench engineer. Then, he joined the mechanical engineering department of INSA where he is now professor. He got his Doctorate of Science in 1993 dealing with the modelling, simulation and control of electrohydraulic actuators. His research activity is focused on aerospace and automotive hydraulic systems.

OLIVIER GEIDER
Master of Science in 1992 at the University of Science in Toulouse. Then, he joined the Laboratoire de Génie Mécanique as a Phd student. In 1997, he presented his Phd dealing with the modelling and control of a low cost pneumatic actuator. Since 1998, he is working as a project engineer on aircraft air conditioning systems at Liebheer Toulouse.

STÉPHANE COLIN
Engineer diploma in 1989 from ENSHEEIT in Toulouse. He presented his Phd in 1992 dealing with the modelling and design of a linearised flapper valve. Since this date, he works as an assistant professor at the mechanical department of the Toulouse University of Science. In the Laboratoire de Génie Mécanique, he focuses his research activity on the modelling of microfluidics systems.